Journal of Thermal Analysis and Calorimetry, Vol. 89 (2007) 2, 601–608

THERMAL AND STRUCTURAL CHARACTERIZATION OF POLY(ETHYLENE-OXIDE)/KERATIN BLEND FILMS

C. Tonin[1*], *A. Aluigi*[1], *C. Vineis*[1], *A. Varesano*[1], *A. Montarsolo*[1] *and F. Ferrero*[2]

[1]CNR-ISMAC, Institute for Macromolecular Studies, Corso G. Pella, 16-13900 Biella, Italy
[2]Politecnico di Torino, Department of Materials Science and Chemical Engineering, Corso Duca degli Abruzzi, 24-10129 Torino, Italy

Blends of poly(ethylene oxide) (PEO) and keratin were prepared with the aim of obtaining bio-compatible materials suitable for film and fibre production. Aqueous keratin solutions, prepared by keratin extraction from wool with urea, *m*-bisulphite and sodium dodecyl sulphates (SDS), filtration and dialysis, were added with different amounts of PEO and solid films were prepared by casting. The addition of SDS prevents protein aggregation.

Morphological, thermal and spectroscopic analysis of the films pointed out that keratin hinders the PEO crystallization process, since a progressive decrease in the size of PEO spherulites is observed and the melting point and the related enthalpy decrease with increasing the keratin content. On the other hand, according to thermal and spectroscopic investigations, PEO seems to interfere with the keratin self-assembling giving the protein a different thermal behaviour.

Keywords: *film casting, keratin, PEO, polymer blends*

Introduction

The use of biopolymers for economic and environmentally sustainable development is currently growing [1], since emerging applications of biomacromolecules range from packaging and industrial chemicals, to medical implant devices and drug delivery systems.

Biodegradability of biopolymers is the base for their applications, and the exploitation of agricultural residues and/or industry processing by-products are obvious sources of low cost bio materials.

Among these, keratins have received little attention in this field till now, although the disposal of fibre by-products from the textile industry, poor quality raw wools not fit for spinning, hairs and feathers from butchery [2], involves environmental and economic complexions, in consideration that an annual crop of more than 3 million tons of keratin [3] has been estimated from data related only to domestic species [4].

Keratin regenerated from wool could find interesting applications in several fields, from biomedical to filtration systems. Films of regenerated wool keratin prepared by casting, degrade in vitro (by tripsin) and in vivo (subcutaneous embedding in mice) suggesting the biocompatibility of keratin [5] and well support fibroblast cell attachment and proliferation [6]. In addition, upon sonication, reduced keratin forms spherical microcapsules which trap solvents or dyes [7]. Moreover, Misra has found that keratin materials are effective adsorbent for heavy metals from aqueous solutions [8].

The fragility and the poor mechanical properties of regenerated keratin restrict processing and application, but large potential application can be envisaged for blends of these proteins with appropriate polymers capable of giving expected performances.

This work is a preliminary study of poly(ethylene-oxide)/keratin systems developed with the aim of producing biocompatible materials, suitable for fibre production by wet-spinning and electrospinning [9].

Keratins are the main constituents of the spindle-shaped long cortical cells making-up 30–60 mass% of the wool fibers [10]. Keratins are distinguished from collagen, silk fibroin and other structural proteins because of their high content of cysteine and half-cystine residues (7–20 mol% of all amino acid residues) which is responsible for the high environment stability [11, 12].

Keratin can be extracted from wool by cleavage of the disulfide and hydrogen inter-chain bonds. Several extraction methods have been reported in literature and most of them involves oxidants or reducing agents like peroxides [13, 14] and thiols [15, 16].

Poly(ethylene-oxide) is a non-degradable polymer capable on packing in crystal. This polymer is often used as an ideal model for a wide variety of studies, and in biomedical applications it is of special interest because of its good compatibility [17] and low toxicity [18].

* Author for correspondence: c.tonin@bi.ismac.cnr.it

1388–6150/$20.00

Akadémiai Kiadó, Budapest, Hungary
Springer, Dordrecht, The Netherlands

In the present work, keratin extracted from wool by sulphitolysis [19] was characterized by gel electrophoresis. PEO/keratin blend films were then prepared with several composition ratios and studied using light microscopy, DSC and FTIR analysis, with the aim of investigating the fine structure gathering knowledge for further processing and applications.

Experimental

Materials

Preparation of keratin solution

Wool fibres were cleaned by Soxhlet extraction with petroleum ether to remove fatty matters, washed with distilled water and conditioned at 20°C, 65% r.h. for at least 24 h.

3 g of cleaned and conditioned fibres were cut and put in 100 mL of aqueous solution containing urea (8 M) and *m*-bisulphite (0.5 M) adjusted to pH 6.5 with NaOH 5 N.

Several extraction methods were tested varying the SDS amount, the temperature and the time of treatment (Table 1). In each experiment, the resulting mixture was quickly filtered (50 mesh) and the filtrate was dialyzed using cellulose tube (molecular mass cut-off 12000–14000 Da) *vs*. distilled water for 3 days. The outer solution was changed three times a day. The insoluble material was removed by centrifugation on centrifugal-driven millipore filter (pore size 5 μm) at 12000 rpm for 15 min. The protein concentration of the dialyzed part was measured by the Bradford protein assay method, using bovine serum albumin as standard. The dialyzed part was concentrated with rotary vacuum evaporator (Buchi Rotavapor R-205) to 1–5 mass%.

The degradation extent of the extracted keratins was controlled by SDS-PAGE analysis.

The turbidity of the keratin solutions was measured at 540 nm using a Perkin Elmer Lambda 40 UV-Vis spectrometer.

Blends preparation

PEO/keratin solutions (5 mass%) of various PEO/keratin ratios were prepared by adding PEO ($4 \cdot 10^5$ g mol^{-1}, supplied by Sigma-Aldrich) into the keratin aqueous solutions. Films of 0.01 mm thickness were prepared by casting from these solutions at 40°C and dried in a desiccators under vacuum, at room temperature.

Methods

Morphological studies

The supramolecular structure of PEO and PEO/keratin blends was investigated by a Leica DM-LP Polarizing Light Microscope.

Differential scanning calorimetry (DSC)

Differential scanning calorimetry measurements were performed by a 821 Mettler Toledo DSC. In order to study the PEO thermal behaviour, the samples, under nitrogen flow of 10 mL min^{-1}, were first heated from 30 to 105°C (I run), at heating rate of 20°C min^{-1}. After 5 min isotherm at 105°C, they were cooled to –60°C at the same rate (II run) and then reheated to 150°C at 10°C min^{-1} (III run).

The thermal behaviour of keratin, was studied by heating the samples from 120 to 400°C at a heating rate of 10°C min^{-1}, under nitrogen flow of 10 mL min^{-1}.

Fourier transform infrared spectroscopy

FTIR spectra were obtained using the ATR technique by a Nexus Thermo Nicolet Spectrometer. Scans were taken with a resolutions of 4 cm^{-1} and gain 8.0.

Results and discussion

Keratin solution

Keratin extraction may take place only after reduction or oxidation of disulfide bonds. The reducing agents

Table 1 Keratin extraction procedures

Method	Extraction solution	Treatment	Yield/mass%	Observation
1	[urea]=8 M [sodium bisulphite]=0.5 M pH=6.5	shaking at 100°C, 1 h	22	degradation of proteins
2	[urea]=8 M [sodium bisulphite]=0.5 M SDS g/wool g=0.3 pH=6.5	shaking at 65°C, 5 h	30	dull solution
3	[urea]=8 M [sodium bisulphite]=0.5 M SDS g/wool g=0.6 pH=6.5	shaking at 65°C, 5 h	33	limpid solution

Table 2 Reduction procedures for the protein extraction from wool

Reducing agents	Urea	pH	Treatment	Yield/%
Mercaptoethanol (1.1 M) [5]	7.4 M	7	shaking at 50°C, 6 h	48
Thioglycolic acid (0.2 M) [14]	8 M	11	shaking at 50°C, 3 h	70
Dithiothreitol (0.2 M) [15]	8 M	11	shaking at 20°C, 16 h	60
m-Bisulphite (0.5 M)	8 M	7	shaking at 65°C, 5 h	33

often used are thiols (thioglycolic acid, dithiothreitol and 2-mercaptoethanol) and they are always used in combination with a protein denaturing agent like urea that breaks hydrogen bonds.

For further scaled-up processes, it is preferable to use sulphitolysis with *m*-bisulphite/urea, although the extraction yield is lower (Table 2), instead of harmful reducing agents.

During sulphitolysis, cystine disulphide bonds are cleaved by sulphite to give cysteine thiol (reduced keratin) and cysteine-S-sulphonate (or Bunte salt) residues [20]:

$$WSSW+SO_3^{2-} \rightarrow WS^- + WSSO_3^-$$

where WSSW is the cross-linked keratin in the fibre, SO_3^{2-} is the sulphite, WS^- is the reduced keratin and $WSSO_3^-$ is the Bunte salt.

The electrophoretical analysis pattern of wool proteins extracted with a reductive buffer is shown in Fig. 1. Two high molecular mass bands (67000–45000 Da) and two low molecular mass bands (28000–11000 Da) are present in the wool fibre trace (line 2) attributed, respectively, to the microfibril and matrix components of the fibres [21]. The electrophoretic patterns of regenerated keratin extracted with the methods described above (Fig. 2), suggest that under mild condition (65°C) S-sulfo keratin does not degrade during the treatments (lines 3 and 4); on the contrary, an extended treatment at 100°C causes a partial protein degradation (line 2).

The effect of the SDS addition in the keratin solution was studied following the protein aggregation through the turbidity change *vs*. time (Fig. 3) [22]. For the lower SDS/keratin ratios, the increase of turbidity occurs in 30 days while the solution with 0.6 SDS/keratin mass ratios showed no turbidity increase. The obtained results suggest that SDS addition during the extraction does not influence the yield (Table 1) whereas aids the stability of the keratin solution.

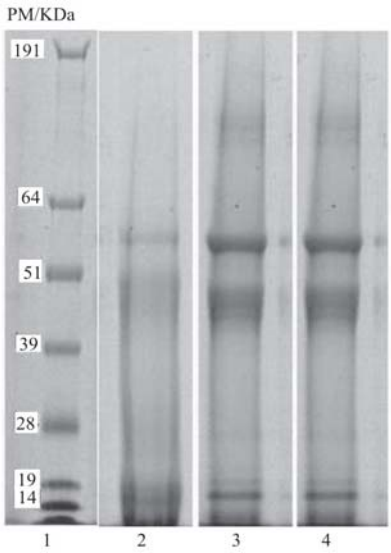

Fig. 2 SDS-PAGE: 1 – standard, 2 – extraction 1, 3 – extraction 2 and 4 – extraction 3

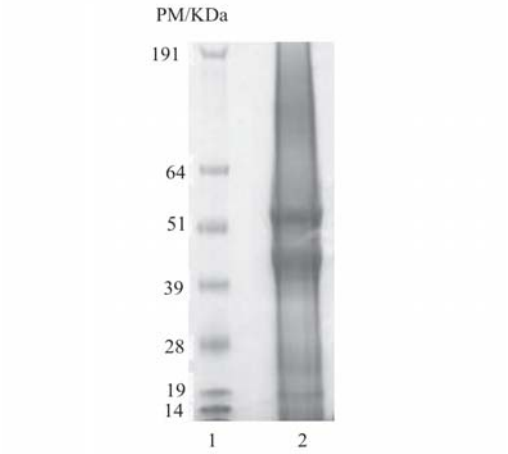

Fig. 1 SDS-PAGE: 1 – standard, 2 – wool

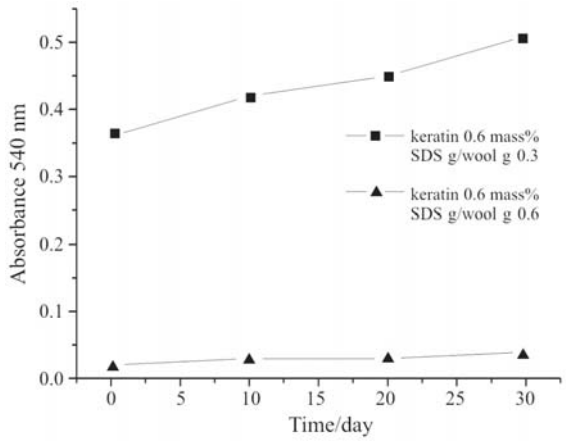

Fig. 3 Turbidity *vs*. time measured at 540 nm

Light microscopy

The films prepared as previously described were transparent, especially those richer in keratin. PEO is a semi-crystalline polymer which in the solid state contains amorphous and crystalline regions where macromolecules exist as double parallel helices arranged as plate-like structures known as lamellae, arranged in spherical structures (spherulites) [23]. Polarized light microscopy investigation shows large crystals in the pure PEO sample, whereas the samples containing 80, 60 and 40 mass% of PEO show a large amount of crystallites with smaller dimension (Fig. 4). Thus, the morphology of the spherulites becomes more irregular with increasing the protein content. The sample with 20 mass% of PEO shows the absence of crystal structures. This suggests that the presence of keratin disturbs the crystallization process, and when the keratin content reaches 80 mass% the crystallization is totally inhibited.

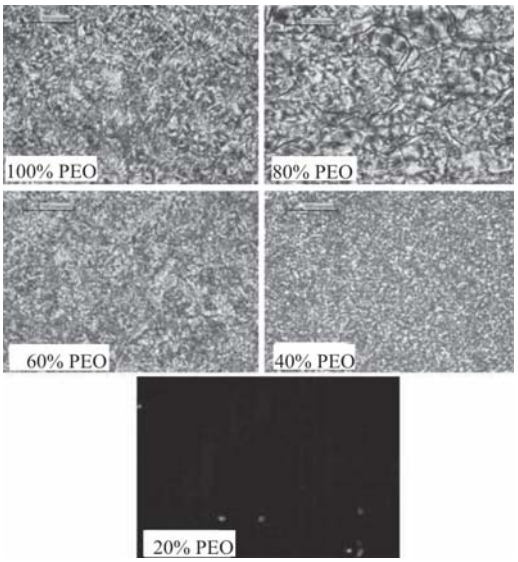

Fig. 4 Polarized light micrographs of the PEO/keratin blend films, ×200, bar represents 100 μm

Differential scanning calorimetry

Figure 5 shows the DSC traces recorded for the second heating scan in the range –60 to 150°C. The thermal properties of the different PEO/keratin blends are listed in Table 3.

The endothermic peaks observed in Fig. 5 are related to the melting point of the PEO crystalline phase in the blends.

The melting temperatures of PEO decrease with increasing the keratin content from 65.5°C for pure PEO to 53.5°C for the sample 40 mass% PEO.

Figure 6 shows the melting enthalpy related to the PEO/keratin system as a function of the blend composition; the line represents the theoretic enthalpy related to PEO melting if the keratin were simply present in the bulk without interfering with the crystalline polymer.

The quick decrease of both the temperature and the enthalpy melting of PEO with increasing the keratin content, suggests that the presence of the protein hinders the crystallization process. Moreover, in Fig. 5, the PEO melting peak disappears in the film containing 20 mass% PEO, indicating that no crystalline structure

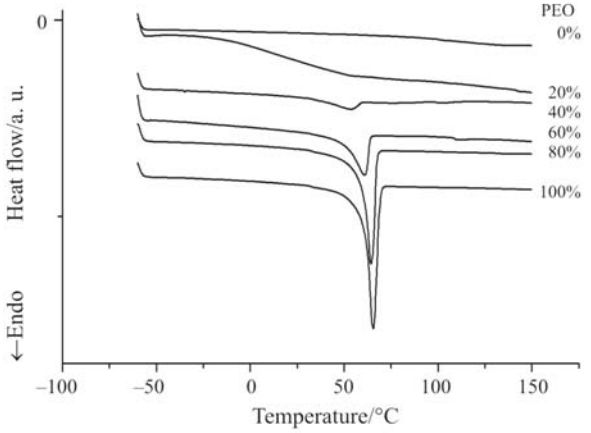

Fig. 5 DSC curves for pure PEO, pure keratin and PEO/keratin blends recorded at the heating rate of 10°C min^{-1} from –60 to 150°C

is formed but a glass transition take place at about 16°C, whilst for pure keratin (0% PEO) the C_p/temperature function is free from thermal effects in the same temperature range. These results are in good agreement with the polarized light microscopy observations.

Finally, the crystallization temperature progressively decreases with increasing the keratin amount

Table 3 Thermal properties of PEO/keratin blends

PEO/%	T_m/°C	ΔH_m^{sper} (blend)/J g^{-1}	ΔH_m^{sper} (PEO)/J g^{-1}	ΔH_m^{theor} (PEO)/J g^{-1}	T_c/°C
100	65.5		130	130	43.6
80	64.4	92.45	115.6	104	41.6
60	60.7	49.85	83.1	78	40.9
40	53.5	13.84	34.6	52	9.7
20	–	–	–	26	–

T_m: melting temperature, T_c: crystallization temperature, ΔH_m: melting enthalpy

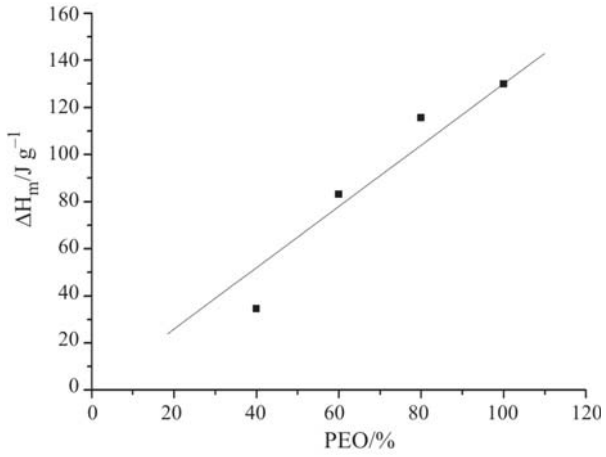

Fig. 6 PEO melting enthalpy as a function of the PEO amount in the PEO/keratin films

(Table 3) suggesting that keratin modifies the kinetics formation of PEO crystals during cooling. No exothermic peaks have been observed indeed for the 20 mass% PEO sample, confirming that no tendency to crystallize was evidenced for samples containing small PEO amounts.

Figure 7 shows the DSC traces recorded in the temperature range from 120 to 400°C. This range includes protein denaturation followed by protein degradation [24, 25]. The thermogram of pure keratin and those of 20 mass% PEO show the peak related to protein denaturation at 212°C, whereas, the protein denaturation shifts to higher temperatures in the 40 and 60 mass% PEO samples (233 and 237°C, respectively). On the other hand, the protein denaturation peak of the sample with the smallest amount of keratin (80 mass% PEO), shifts at a lower temperature (194°C) than those of pure keratin. This behavior suggests that PEO interferes with the keratin self-assembling causing the protein to assume a secondary structure thermally more stable for balanced blends, but an excess of

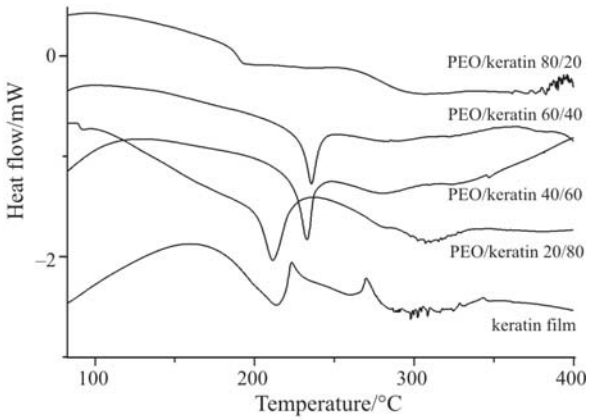

Fig. 7 DSC curves for pure keratin and PEO/keratin blends recorded at the heating rate of 10°C min^{-1} in the range from 30 to 400°C

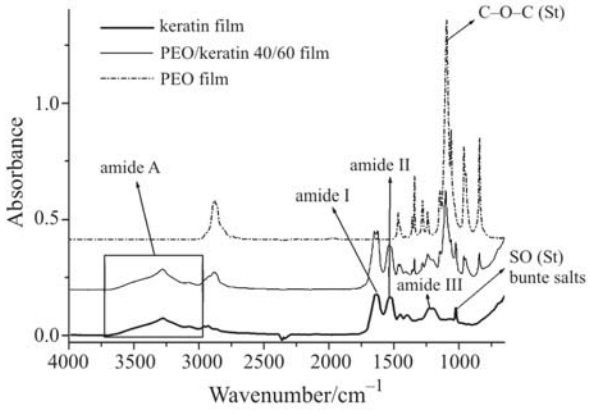

Fig. 8 Infrared spectra of pure PEO, pure keratin and 40/60 PEO/keratin blend film as example

PEO leads back the protein chains to organize in a thermally less stable secondary structure.

FTIR analysis

As regards FTIR spectrum of the protein component (Fig. 8), keratin shows a wide absorption band in the 4000–2800 cm^{-1} range known as amide A. This band is not amenable for qualitative and quantitative evaluation because it contains 9 vibrational overlapped modes [26]. However, keratin presents most important absorption bands in the region below 2000 cm^{-1} such as amide I (1635 cm^{-1}), amide II (1528 cm^{-1}) and amide III (1230 cm^{-1}), and the band at 1020 cm^{-1} related to SO stretching vibration of Bunte salts residues [27]. Particularly, amide I absorption, which arises primarily from the C=O stretching vibration of amide carbonyl groups, has been shown to be sensitive to the protein secondary structures. In fact, it includes a wide distribution of C=O stretching frequency depending on a variety of protein secondary structures [28, 29]. Fortunately, because the amide I region is not affected by PEO absorptions, information on the previously described arrangements of the protein chains, due to the presence of different amount of PEO in the blends, can be gathered by studying related shape changes of this band.

The broad amide I bands of all samples were normalized and resolved by the second order derivative; it should be noted that the peak positions are inverted in the second order spectra (Fig. 9).

On the basis of literature data, the absorption peak at 1650 cm^{-1} suggests the presence of an α-helix structure in the keratin chains, whereas the component at 1621 cm^{-1} indicates the presence of β-sheet type arrangements; bands in the 1680–1695 cm^{-1} region indicate the existence of disordered protein structures [30]. Therefore, the second order derivative amide I related to the pure keratin film (Fig. 9a) suggests the presence of both α-helical conformation and β-sheet secondary

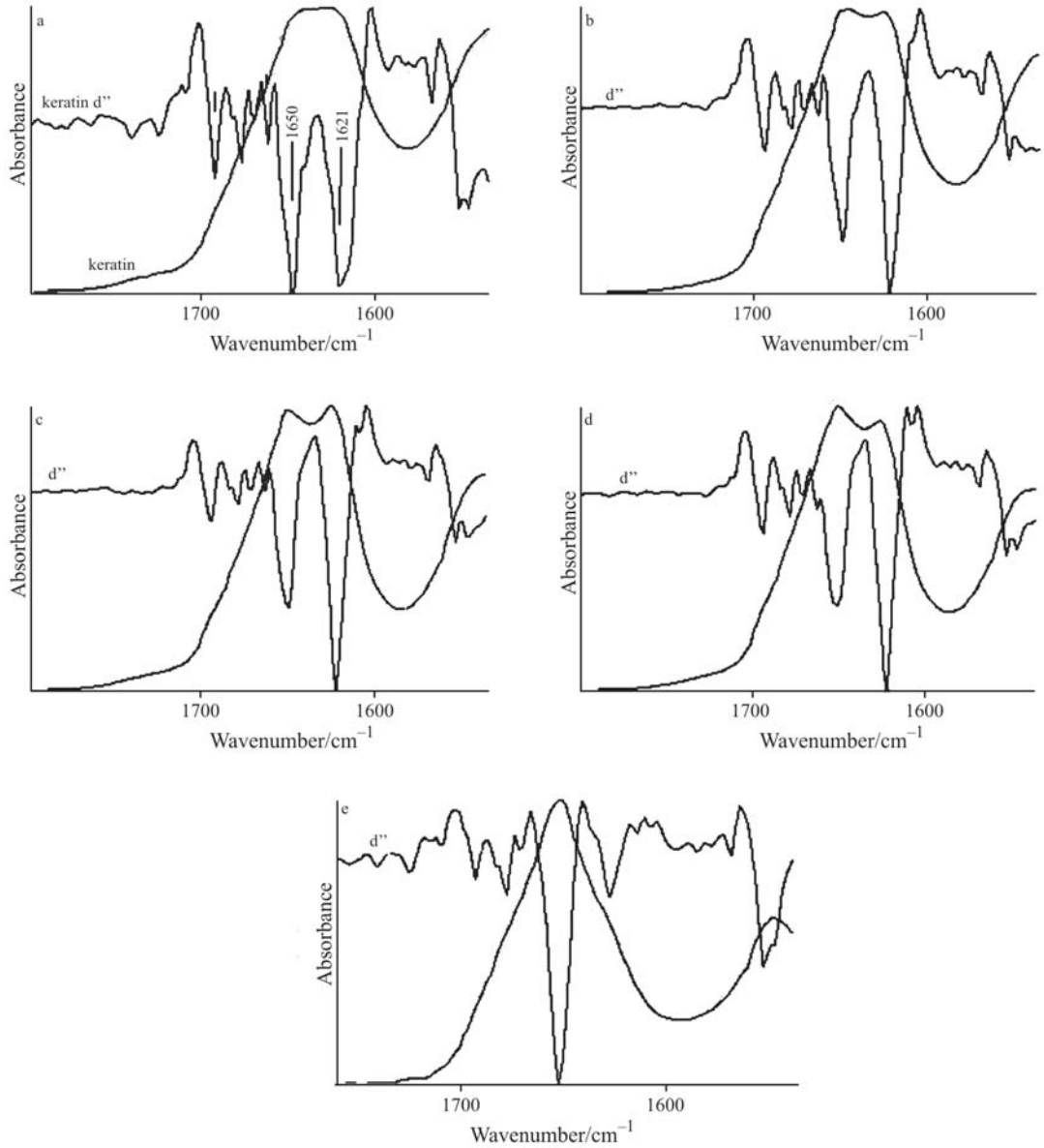

Fig. 9 Infrared spectra and related second order derivative in amide I region of pure keratin and PEO/keratin blend films; a – keratin, b – PEO/ker 20/80, c – PEO/ker 40/60, d – PEO/ker 60/40 and e – PEO/ker 80/20

structure. The sample 20 mass% PEO (Fig. 9b) film has the same behaviour.

On the other hand, in the samples 40 and 60 mass% PEO (Figs 9c and d) the peak related to β-sheet structure increases with respect to the α-helix absorption. Finally, the amide I second order derivative of the 80 mass% PEO sample suggests a significant proportion of α-helical conformation with a lesser degree of β-sheet structure (Fig. 9e).

Therefore, the presence of PEO seems to give stability to the keratin β-sheet structure, that it is known to be thermally more stable, according to DSC analysis. But, when the keratin is surrounded by a large amount of PEO such as in the 80 mass% PEO sample, most protein tend to assume the α-helix conformation that denatures at lower temperature, according to the thermal behaviour [31].

As regard of the synthetic polymer, the presence of a crystalline PEO phase is confirmed by the triplet peak of the C–O–C stretching vibration at 1145, 1094 and 1059 cm^{-1}, with the maximum at 1094 cm^{-1} (Fig. 10) [32]. The increase in the wavenumbers of the C–O–C stretching from 1094 cm^{-1} for the pure PEO sample to 1102 cm^{-1} for 40 mass% PEO sample is observed with increasing the keratin content. Changes in the shape and position of this absorption peak could be due to PEO crystalline phase changes in the different blends. The disappearance of the triplet shape of the C–O–C absorption band in the blend with 20 mass% PEO indicates the absence of a PEO crystalline structure, in agreement

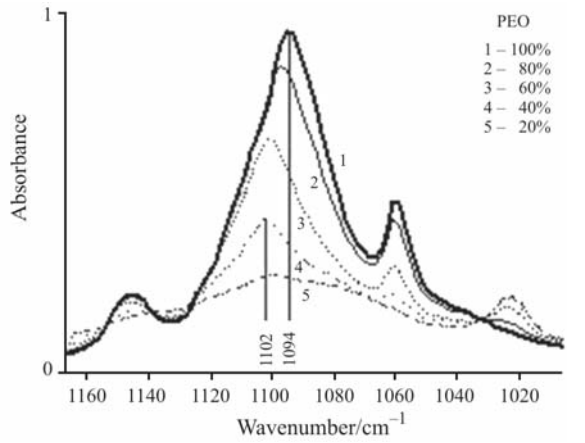

Fig. 10 Infrared spectra in the C–O–C stretching vibration region of pure PEO and PEO/keratin blend films

with the previously described results from morphology and thermal analysis.

Conclusions

When wool keratin is extracted in aqueous solutions of *m*-bisulphite and urea, the addition of SDS to the extraction medium prevents protein aggregation, making the keratin solution more stable without significantly influencing the extraction yield. SDS-PAGE analysis shows that an extended treatment at 100°C causes a partial protein degradation, whereas keratin extracted at 65°C is well preserved.

Transparent and solid PEO/keratin films were prepared by casting from aqueous solutions of the two polymers in several blending ratios. The transparency is enhanced with increasing the protein content.

Morphological, thermal and spectroscopic analysis pointed out that the two polymers interfere each other in the supramolecular arrangements. In particular, keratin hinders the PEO crystallization decreasing the spherulites size, the melting point and the related enthalpy. In addition, keratin affects the formation kinetics of PEO crystals during cooling, the DSC curves showing a decrease of the crystallization temperature with increasing the protein amount.

On the other hand, DSC and FTIR analyses highlighted that PEO interferes with the keratin self-assembling, giving the protein a different thermal behaviour. Particularly, in the samples with comparable amount of PEO and keratin, PEO seems to stabilize the thermally more stable β-sheet conformation. Whereas, when the PEO amount overcomes keratin, the protein chains tend to organize in the α-helix structure that is a thermally less stable secondary structure.

PEO/keratin blends appear as promising candidates for the production of new bio-compatible materials suitable for a number of applications in different areas, ranging from medical applications (scaffolds, drug delivery membranes), to filtration and absorption equipments, by film casting, electrospinning and conventional wet-spinning techniques.

Acknowledgements

We thank Fondazione Cariplo for the financial support of this program.

References

1 H. G. Fritz, T. Seidenstucker, U. Bolz, M. Juza, J. Schroeter, H. J. Endres, H. G. Fritz, T. Seidenstucker, U. Bolz, M. Juza, J. Schroeter and H. J. Endres, Eds, European Commission, DG-XII, Science, Research and Development, 1994.
2 E. Salminen and J. Rintala, Bioresource Technol., (2002) 13.
3 F. Garzena, Degree Thesis, Politecnico di Torino, Torino, Italy 2003.
4 R. W. Moncrieff, Man Made fibres, 6th Ed., Butterwhorths Scientific, London 1975, Vol. 11, p. 231.
5 K. Yamouchi, A. Yamauchi, T. Kusunoki, A. Kohda and Y. Konishi, J. Biomed. Mater. Res., 31 (1996) 439.
6 K. Yamouchi, M. Mniwa and T. Mori, J. Biomater. Sci. Polym. Ed., 9 (1998) 259.
7 K. S. Suslick and M. W. Grinstaff, J. Am. Chem. Soc., 112 (1990) 7807.
8 M. Misra, P. Kar, E. C. Homonoff and C. Licata, 'AKF' Keratin-Protein Fiber as a bisorbent for heavy metals from solutions. American Filtration and Separation Society Annual Meeting, Tampa, FL, April 30–May 4, 2001.
9 C. Vineis, A. Aluigi, A. Montarsolo, A. Varesano, G. Mazzuchetti, C. Tonin and F. Ferrero, 'Nanofibres of wool keratin/poly-ethylene-oxide blends for biomedical applications', in Proc. 6th Textile and Health Int. Forum, 4–5 May 2006, Biella, Italy.
10 Wool Handbook; W. Bergen, Interscience Publishers, London England 1963, Vol. 1, p. 137.
11 J. H. Bradbury, Adv. Protein Chem., 27 (1973) 111.
12 R. D. B. Fraser, T. P. MacRae, G. E. Rogers and C. Charles, Thomas Publisher, Springfield 1972.
13 J. M. Gillespie, I. J. O'Donnell, E. O. P. Thompson and E. F. Woods, J. Text. Inst., 51 (1960) 703.
14 E. O. P. Thompson and I. J. O'Donnell, Aust. J. Biol. Sci., 12 (1959) 282.
15 J. M. Gillespie and F. G. Lennox, Aust. J. Biol. Sci., 8 (1955) 97.
16 J. A. MacLaren, Text. Res. Inst., (1987) 87.
17 N. P. Desai and J. A. Hubbel, Biomaterials, (1991) 12.
18 J. E. Bergsma, F. R. Rozema, R. R. M. Bos, W. C. de Bruijn, G. Boering and A. J. Pennings, Biomaterials, (1995) 16.
19 C. R. Robbins, Chemical and physical behaviour of human hair, 2nd Ed., Springer-Verlag, New York–Berlin.
20 J. A. MacLaren and B. Milligan, Wool Science Science Press, 1981, p. 35.
21 J. A. MacLaren and B. Milligan, Wool Science Science Pess, 1981, p. 1.

22 P. M. M. Schrooyen, P. J. Dijkstra, R. C. Oberthur, A. Bantjes and J. Feijen, J. Colloid Interface Sci., 240 (2001) 30.
23 P. J. Sanchez-Soto, J. M. Gines, J. M. Arias, Cs. Novák and A. Ruiz-Conde, J. Therm. Anal. Cal., 67 (2002) 189.
24 M. Spei and R. Holzem, Melliand Textilberichte, 6 (1991) 431.
25 Zs. Éhen, Cs. Novák, J. Sztatisz and O. Bene, J. Therm. Anal. Cal., 78 (2004) 427.
26 K. Gribenow, A. M. Santos and K. G. Carrasquillo, The Internet Journal of Vibrational Spectroscopy, 3 (2002) edition 1, 1.
27 F. J. Douthwaite and D. M. Lewis, JSDC, 10 (1994) 304.
28 W. K. Surewics, H. H. Mantsch and D. Chapman, Biochem., 32 (1993) 389.
29 D. J. Lyman, J. Murray-Wijelath and M. Feughelman, J. Appl. Spectrosc., 55 (2001) 552.
30 M. G. Sowa, J. Wang, Ch. P. Schultz, M. K. Ahmed and H. H. Mantsh, Vib. Spectrosc., 10 (1995) 49.
31 C. Tonin, A. Aluigi, M. Bianchetto Songia, C. D'Arrigo, M. Mormino and C. Vineis, J. Therm. Anal. Cal., 77 (2004) 987.
32 X. Li and Sl. Hsu, J. Polym. Sci. Polym. Phys. Ed., 1984, pp. 22–1331.

Received: February 24, 2006
Accepted: May 17, 2006
OnlineFirst: October 20, 2006

DOI: 10.1007/s10973-006-7557-7